

IAC-19-A2.6.2

In situ observation of growth dynamics in DECLIC Directional Solidification Insert onboard ISS: DSI-R flight campaign**F.L. Mota^{a*}, K. Ji^b, T. Lyons^c, L.L. Strutzenberg^d, R. Trivedi^c, A. Karma^b, N. Bergeon^a**^a *IM2NP, Aix-Marseille Université and CNRS, Marseille, France*^b *Physics Department, Northeastern University, Boston, USA*^c *Department of Materials Science & Engineering, Iowa State University, USA*^d *Marshall Space Flight Center, Huntsville, USA** Corresponding Author: fatima.mota@im2np.fr**Abstract**

The study of solidification microstructure formation is of utmost importance for materials design and processing, as solid-liquid interface patterns largely govern mechanical and physical properties. Pattern selection occurs under dynamic conditions of growth in which the initial morphological instability evolves nonlinearly and undergoes a reorganization process. The dynamic and nonlinear nature of this instability renders in situ observation of the interface an invaluable tool to gain knowledge on the time-evolution of the interface pattern. Transparent organic analogs, which solidify like metallic alloys, allow direct visualization of interface dynamics. Extensive ground-based studies of both metallic and organic bulk samples have established the presence of significant convection during solidification processes that alters the formation of interfacial microstructures. A reduced-gravity environment is therefore mandatory for fluid flow elimination in bulk samples. In the framework of the CNES project MISOL3D (MICrostructures de SOLidification 3D) and the NASA projects DSIP (Dynamical Selection of 3D Interface Patterns), SPADES (SPAtiotemporal Evolution of three-dimensional DEndritic array Structures) and CAMUS (ComputAtional Studies of MicrostrUcture Formation During Alloy Solidification in Microgravity), we participated in the development of the Directional Solidification Insert (DSI) of the DEvice for the study of Critical Liquids and Crystallization (DECLIC). The DECLIC-DSI is dedicated to in situ and real-time characterization of solid-liquid interface patterns during directional solidification of transparent alloys in diffusive transport regime. Between April 2010 and March 2011, the first ISS campaign (DSI) explored the entire range of microstructures resulting in unprecedented observations. A second campaign (DSI-R), performed between October 2017 and December 2018, in which the insert contained an alloy of higher solute concentration, allowed to complete the benchmark database. The increase of solute concentration resulted in well-developed dendritic patterns at lower velocities (lower interface curvature and larger tip radius). The microstructure resulting from dendritic growth is dominant in metallurgy so that it is fundamental to understand the mechanisms of its formation. The main aims of this experimental campaign are to understand: the mechanisms of the cell to dendrite transition, the fundamental mechanisms of sidebranching formation, the dependence of dendrite tip shapes on growth conditions, the interaction of primary array and secondary sidebranches, and the influence of subgrain boundaries on the spatiotemporal organization of the array structure. Preparation, analysis and interpretation of the experiments performed onboard ISS are considerably enhanced by experiments performed on ground using thin-samples (Pr. Trivedi's group) and phase-field simulations of microstructure formation in a diffuse growth regime (Pr. Karma's group). In this summary, we will present an initial assessment of the results obtained during the DSI-R campaign.

Keywords: DECLIC, Solidification, microgravity, transparent alloys, dendritic regime**Nomenclature**

V_p : pulling velocity
 G : thermal gradient
 L : solidified length
 r_{tip} : tip curvature radius

Acronyms/Abbreviations

CADMOS: Centre d'Aide au Développement des activités en Micro-pesanteur et des Opérations Spatiales
 CNES: Centre National d'Études Spatiales

DECLIC: Device for the study of Critical Liquids and Crystallization

DSI: Directional Solidification Insert

DSI-R: Directional Solidification Insert - Refurbish

ISS: International Space Station

NASA: National Aeronautics and Space Administration

PF: phase-field

SCN: Succinonitrile

3D: three-dimensional

1. Introduction

The study of solidification microstructure formation and selection is crucial to engineering and the processing of advanced new materials. The most common microstructures are cells and dendrites, which form the interface solidification patterns that largely govern mechanical and physical properties of materials. The evolution of these microstructures occurs under dynamic conditions, in which the pattern self-organizes into a rather periodic array. Therefore, *in situ* and real time observation of the solid-liquid interface is an important tool to study the time-evolution of the interface. In light of this, transparent organic analogues that behave like metallic alloys are extensively used.

Unfortunately, the strong influence of convection on the solidification interface is a critical impediment in the study of three-dimensional pattern evolution in ground-based experiments. Extensive ground-based studies carried out in metallic and organic bulk samples have clearly established that fluid flow modifies the solute boundary layer, influencing the pattern development [1, 2].

Directional solidification experiments under low gravity conditions provide a unique framework to investigate microstructure development in spatially extended sample geometries, with negligible convection effects and under well-controlled conditions of growth rate, temperature gradient, and alloy composition. The study presented here was conducted using the DSI dedicated to *in situ* and real time characterization of the dynamical selection of the solid-liquid interface morphology in *bulk* samples of transparent materials, which was developed by the CNES in the frame of the DECLIC project. The DECLIC facility of CNES was launched for the first time with 17-A shuttle flight (August 2009) as part of a joint NASA/CNES research program and was installed on the ISS in microgravity environment. The main instrument monitoring is performed from the CADMOS in Toulouse. Taking advantage of provided tele-science capabilities, scientists have the ability to follow and remotely control experiments. The DSI was commissioned in December 2009, and 51 experiments during six runs of two to three weeks each were performed from April 2010 to April 2011. The DSI was then brought back on ground and two runs of two weeks have been performed at the CNES with similar control parameters to experiments in microgravity so that convection influence could be addressed [3, 4]. A second ISS campaign of DSI, DSI-R, took place between October 2017 and November 2018, on a sample of higher composition that allows exploring widely the microstructure map as function of the control parameters and thereby completing the reference database in diffusive regime: 50 experiments during six runs of three weeks.

The first ISS campaign DECLIC-DSI, performed using a SCN-0.24wt% camphor alloy, was very successful, and allowed to explore the entire range of microstructures, from planar front to cells and dendrites. After the return of DSI on Earth, selected experiments were performed on Earth under gravity-driven fluid flow to evidence convection effects. Both radial and axial macrosegregations are observed on ground experiments, and primary spacings measured on Earth and microgravity are considerably different. The reduced gravity environment of space provides unique benchmark data for numerical simulations of spatially extended patterns under diffusive growth conditions [4]. A thorough analysis of the initial recoil of the planar solid-liquid interface within the temperature field, as the sample is pulled towards the colder region from its initial *liquidus* position, shed light on complex thermal conditions within the experimental setup [5]. In order to properly reproduce the transient interface dynamics, one needs to account for two thermal effects: (i) finite heat transport inside the sample within the adiabatic zone, and (ii) latent heat rejection as the liquid solidifies. Accounting for these thermal effects leads to a major improvement in the agreement between (3D) phase-field simulations and microgravity measurements for both the time of occurrence of morphological instability after the start of the experiment and the subsequent spacing evolution, which are not accurately predicted using the standard frozen temperature approximation [6]. The favorable conditions provided by microgravity also allowed to observe for the very first time the dynamics of extended oscillating cellular patterns that were also further investigated by three-dimensional (3D) phase-field simulations [7-9]. The characteristics, the spatio-temporal coherence and the conditions of existence (or inhibition criteria) of these oscillating patterns were evidenced. In 3D extended patterns, the cell oscillations are generally not coherent over spatially extended regions of many cells. The phase-field simulations showed that this lack of coherence arises from tip splitting events that occur when the oscillation amplitude exceeds a threshold and cause the cellular array to be spatially disordered. Phase-field simulations also showed that oscillations can be coherent over large scales only in the absence of tip splitting and for special initial conditions corresponding to a perfectly ordered hexagonal array, which is typically not dynamically selected experimentally. Work is still on progress on the DSI results and it focuses on the influence of crystal misorientation with respect to the thermal gradient on the primary spacing adjustment and the evolution of subgrain boundaries as well as their influence on microstructure selection.

The DSI-R campaign was focused on the study of the formation of well-developed dendritic patterns, the dendritic microstructure being of major importance in

metallurgy. Dendritic structures are the predominant microstructural constituents of solidified alloys. The microstructural scales of dendrites, such as primary and secondary arm spacings, control the segregation pattern that largely determines the properties of the material [10]. In order to obtain developed dendritic patterns in the range of low pulling rates, and consequently reduced interface curvatures, this second ISS campaign was performed using a solutal alloy composition higher than in the first one (SCN-0.46wt% camphor). The dendritic regime is characterized by structure tips more parabolic (needle shape), as well as by the appearance of secondary branches; the crystallographic anisotropy becomes particularly visible due to the growth of dendritic branches (primary and secondary) along the preferred crystallographic directions (higher surface energy) [11]. The DSI-R studies focus in particular on the cell-dendrite transition, the secondary branching mechanisms and the dendrite geometrical characteristics as function of growth parameters.

The result of each experiment is a huge amount of images that have to be analyzed to quantitatively characterize the dendritic pattern and its time evolution. In section 2, we will describe the experimental framework before introducing, in section 3, the image procedures developed to analyze the experimental data. In section 4, we will present an initial assessment of the results obtained during the DSI-R campaign. We will finish with some conclusions and perspectives.

2. Directional Solidification Experiments

The DECLIC-DSI consists of a Bridgman type furnace and the experimental cartridge. More thorough descriptions of DECLIC and its inserts can be found in [12, 13]. The experimental cartridge includes a quartz crucible and a system of volume compensation made of stainless steel that is useful to accommodate the sample volume variations associated to phase changes. The cylindrical crucible has an inner diameter of 10 mm and a length that enables about 10 cm of solidification, allowing the study of the entire development of extended 3D patterns, from the initial stage to the steady state. The crucible is equipped with a flat glass window at the bottom and a lens immersed in the melt at the top.

The cartridge was filled under vacuum with a succinonitrile (SCN) – 0.46 wt% camphor alloy, using SCN purified by NASA through distillation and zone melting. Once sealed, the cartridge was inserted in the Bridgman furnace. A monocrystalline seed with a direction $\langle 100 \rangle$ parallel to the pulling axis was prepared on ground and kept during all the experimental campaign.

The hot and cold zones of the Bridgman furnace were setup in a way to impose a thermal gradient ranging from 10 to 30 K/cm and to maintain the solid-

liquid interface in the “adiabatic area” located between the cold and hot zones. During the experiment, the crucible was pulled down from the hot zone into the cold zone at a rate ranging from 0.1 to 30 $\mu\text{m/s}$. For a given alloy concentration, we can set either the thermal gradient or, more conveniently, the pulling rate, to create various interface morphologies, ranging from planar front to cellular and finally dendritic patterns.

Figure 1 shows a representation of the optical apparatus, where the experimental cartridge is reduced to a cylinder with the liquid on top and solid at the bottom. The main observation mode (axial observation) takes advantage of the complete axial transparency of the cartridge: the light coming from LEDs passes through the cartridge from the bottom to the top, therefore crossing the interface. The optical imaging system formed by the immersed lens and a following relay lens forms the image of the interface on a CCD camera. On the same cartridge axis, a He-Ne Mach-Zehnder interferometer is also present, detailed in [14, 15]. The interface can also be observed from the side (transverse observation). The axial direct observation gives information about the microstructure nature and morphology; the axial interferometric observation allows the 3D reconstruction of microstructures and thus to reach its radius of curvature as well as the dynamics of formation of the secondary branches; the transverse observation gives information about the position and shape of the solid-liquid interface. In presence of a macroscopically convex interface and “big” dendrites, the high frequency acquisition of transverse images is an alternative method to observe the dendrite tips.

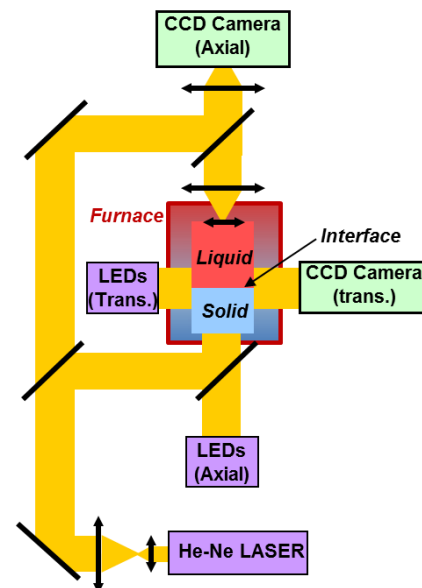


Fig. 1. Representation of the optical apparatus of the DECLIC-DSI.

3. Post-processing

The resulting raw data are a sequence of images of the interface during solidification, including the onset and stabilization of the solidification front. To study the microstructural evolution of the solidification interface, we characterize each dendrite in terms of its position on the interface and its size. Image treatment and analysis procedures have been developed using several software packages (such as Visilog®, ImageJ or Python) to facilitate exploitation of results. We take the axial images and create a binary mask where each dendrite is separately labelled, so that the center of each dendrite can be calculated. A Voronoi tessellation of these points is then used to identify the first neighbors of each dendrite at a given time and to calculate its primary spacing (i.e. average center-to-center distance with first-neighbor dendrites in top-view images). The labels of each dendrite are associated across images, so that it can be followed through the successive images, and its creation, movement, and elimination characterized. Figure 2a shows an example of enhanced contrast image where the skeleton is superimposed.

Throughout the sequence of directional solidifications, macroscopic shape and motion of the interface have been investigated by side view observation. In the case of convex interface with microstructures, the positions of the borders and the center are easily measured corresponding to the dendrite tip position; in case of concave interface, the tip positions in the center can no longer be determined as they are hidden by microstructures located on the border of the crucible. More details are given in [5].

Some particular experiments where the interface was macroscopically convex and the dendrites were well developed allowed the use of transverse images to draw the tip profile and determine the tip radius. An example of transverse raw image is given in Figure 2b with a zoomed region focused on a dendrite tip.

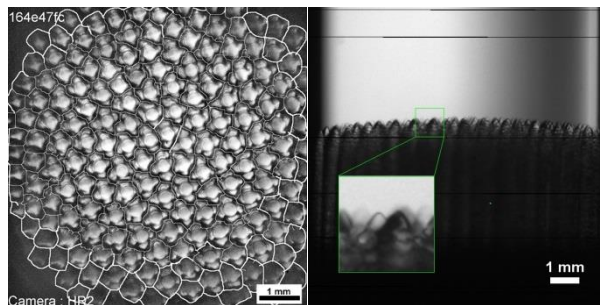


Fig. 2. Direct observation of the solid-liquid interface: (a) axial view with superimposed skeleton obtained after processing; (b) transverse view of a macroscopically convex interface with a zoom on dendrite tips which can be drawn and the tip radius obtained.

4. Results and Discussion

During the DSI-R campaign, 6 experimental runs of 3 weeks were performed which allowed to explore the experimental matrix using the two thermal gradients previously used during the DSI campaign (12 and 19 K/cm), at pulling rates ranging from 0.5 and 12 $\mu\text{m/s}$.

The main objectives of the DSI-R campaign were:

- the acquisition of benchmark data on microstructure formation in diffusive transport conditions and the determination of the microstructure map as a function of experimental control parameters;
- the study of the mechanisms of primary spacing selection and influence of the experimental path on the pattern characteristics;
- the characterization of the dendrite tip shape;
- the study of the conditions and characteristics of side-branching formation.

In order to attain these objectives, different types of experiments were performed:

- for one selected gradient, long solidifications at constant pulling velocity, varying the velocity between experiments;
- for one selected gradient, solidifications with different kind of pulling rate jumps (half-way at $V_{p,1}$ and the remaining at $V_{p,2}$).

The types of analyses performed include:

- the characterization of microstructure type;
- the characterization of the pattern characteristics as function of time (primary spacing and organization);
- the characterization of tip radius and formation of sidebranching;
- the analysis of sub-grains interaction mechanisms (misorientation, competitions);
- the front recoil analysis that corresponds to the tip position, and which can provide evidence of residual macrosegregation [5].

The microstructure formation is quite similar regardless the type of experiments. It will be described on the basis of one experiment shown in Figure 3. The initial interface corresponds to $t = 0$ and $V_p = 0 \mu\text{m/s}$ (Fig. 3a). After triggering of the pulling, morphological instability initiates by forming linear ridges along sub-boundaries that finally underline a rather complex array (Fig. 3b). Between these defects, in interface areas that are still smooth, some circular undulations of the interface (poxes) may be present. Ridges underlying sub-grain boundaries progressively emit new ridges in their transverse direction and, simultaneously, a uniform corrugation that corresponds to the earliest visible wavelength of morphological instability pervades the interface (Fig. 3c). The amplitude of all these interface modulations increases and grooves start to form, but it is

still difficult to identify cells or dendrites (Fig. 3d). At this stage, the interface dynamics is remarkably fast and pattern disorder high. There is then a progressive decrease of disorder and a clear pattern of cells/dendrites eventually emerges (Fig. 3e). The dynamics then slows down and is limited to progressive size adjustment and array ordering (Fig. 3f).

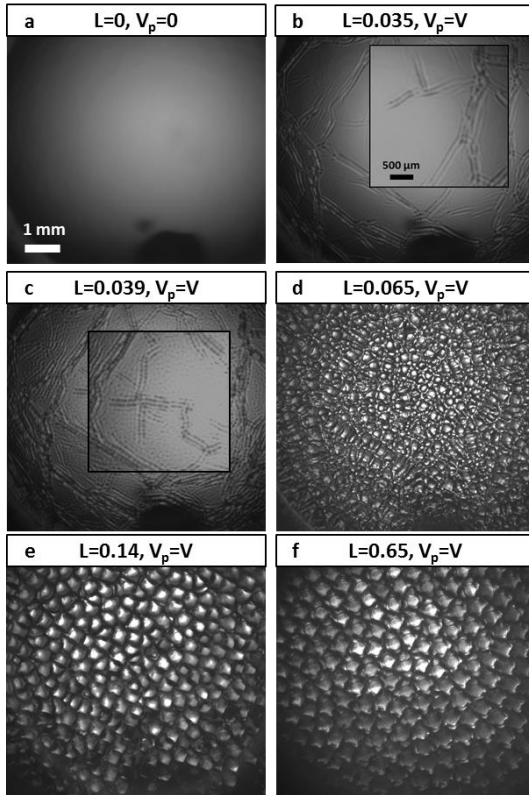


Fig. 3. Typical sequence of formation of the interface microstructure at given pulling rate V and thermal gradient. L denotes the ratio between the solidified length and the total length of the crucible.

Preliminary analysis of each type of experiment will be described in the sections below.

4.1 Solidification of the entire cartridge at constant pulling rate

This kind of experiment aims to complete the benchmark database on microstructure formation and to build a microstructure map as a function of the control parameters. At rest, the solid-liquid front is planar; after imposing a pulling velocity, the interface will destabilize and evolve until attaining a stationary state where the growth velocity is equal to the imposed pulling velocity. The possibility of *in situ* visualization of the solidification allows the characterization of the patterns as function of time. The primary spacing, one of the most fundamental characteristics, is for example followed as function of time, and represented in Figure

4. Several experiments were performed at different pulling velocities and one can notice an important pulling velocity effect. Figure 4 shows three different observed behaviors: at V_1 the primary spacing continuously increases without attaining a steady-state; at V_2 the primary spacing increases monotonically towards its steady-state; at V_3 a peak spacing value is observed before it slowly decreases towards a steady-state value. Similar behaviors were previously observed on cellular patterns during the DSI flight campaign [6, 16].

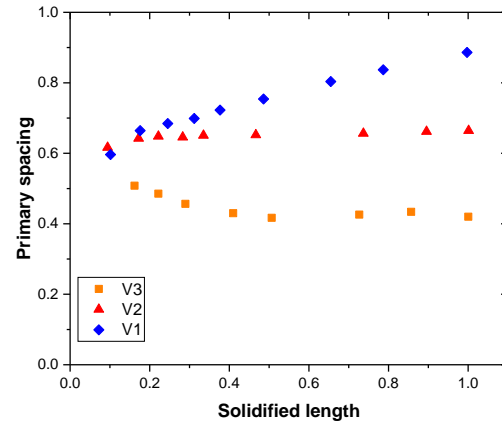


Fig. 4. Primary spacing evolution as a function of the solidified length for different pulling rates ($V_3 > V_2 > V_1$). The primary spacing and the solidified length were normalized by the maximal primary spacing attained (considering all the performed experiments) and the crucible length, respectively.

For the conditions showed in Fig. 3, the axial image acquisition frequency allowed to measure the natural frequency of sidebranching, and given that the dendrites are “big” and the interface macroscopically convex, the side view images allowed to measure the dendrite tip radius. Even if the primary spacing is the most visible shape parameter in our experiments, the dendrite tip radius is the key length scale for solute microsegregation that controls the final properties of the solid material. In order to establish a benchmark database, all pattern characteristics are essential.

Figure 5 shows an example of the solid-liquid interface at the end of solidification for a pulling velocity 4 times higher than the represented in Fig.3. Clearly, the primary spacing is lower than the one represented in Fig.3, and one can notice the existence of several slightly misoriented sub-grains. During the *in situ* and real time monitoring of the solidification experiments, pattern gliding was identified which is associated to the crystal misorientation with respect to the thermal gradient. The different sub-boundaries identified provide interesting data related to grain interactions.

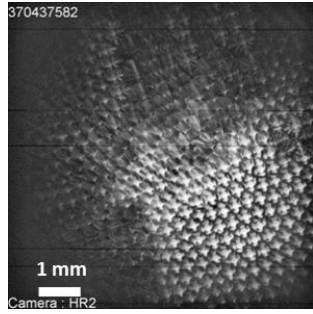


Fig. 5. Axial observation of the solid-liquid interface at the end of solidification for a pulling velocity 4V.

As mentioned in the Post-processing section, the macroscopic motion of the interface was followed by side view observation. Figure 6 shows the evolution of the interface position in the “adiabatic area” as the growth progresses, more exactly as a function of the dimensional solidified length, for a set of different pulling rates and a fixed thermal gradient. These curves characterize the front recoil: they describe the evolution of the interface temperature but may also be influenced by possible thermal field evolutions.

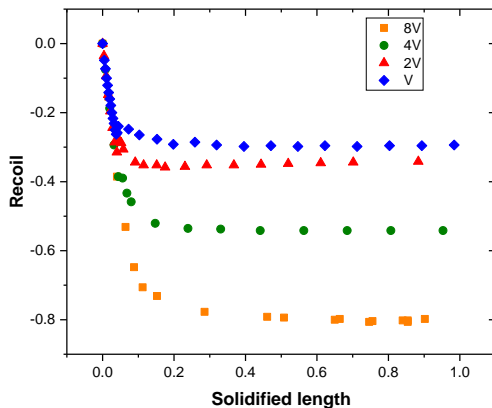


Fig. 6. Front recoil evolution as a function of the solidified length for different pulling velocities. The front recoil and the solidified length were normalized by the maximal recoil attained (considering all the performed experiments) and the crucible length, respectively.

All the curves start with a transient stage, roughly lasting the first 10% of the growth, before reaching a steady-state stage, characterized by a fixed position of the interface in the “adiabatic zone”. The total recoil increases with pulling rate which is not compatible with a frozen thermal field condition. We had previously shown experimentally and by phase-field simulations [5, 6] that complex thermal conditions affect the stationary position of the solid-liquid interface, as well as its dynamics of relaxation towards this stationary

position over a finite time after the onset of sample pulling. The results obtained during this second flight campaign confirm the results previously obtained.

4.2 Solidification with pulling rate jump

The objective of this kind of experiments is to study the dynamics of primary spacing selection, the “history-dependence” of primary spacing “selection” as well as the stability limits. During solidification with pulling rate jumps and depending on the importance of the jump, the pattern may select a different spacing (when compared to long solidification at constant velocity): if the second velocity is higher (lower) than the first, a lower (larger) primary spacing may be selected. The primary spacing needs a significant delay to adjust after the velocity jump, to tend towards its stable value. Figure 7 shows the effect of a step-change in pulling velocity half way through the solidification on the primary spacing and the final microstructure. The red curve shows the slow adjustment of the pattern toward a smaller spacing coming from a lower velocity (step-up). On the blue curve, coming from a higher velocity (step-down), we can see that the spacing does not evolve after the jump but remains significantly lower than the one obtained in the green curve starting from rest at V. The mechanisms of spacing adjustment in our extended 3D patterns also need to be clarified. Classically in ideal patterns, adjustment proceeds by homogenous eliminations, tip-splitting or tertiary branching [17-20]. But we have already point out the fact that our patterns are far from being ideal, presenting numerous defects that may have major influence in these adjustment mechanisms [21].

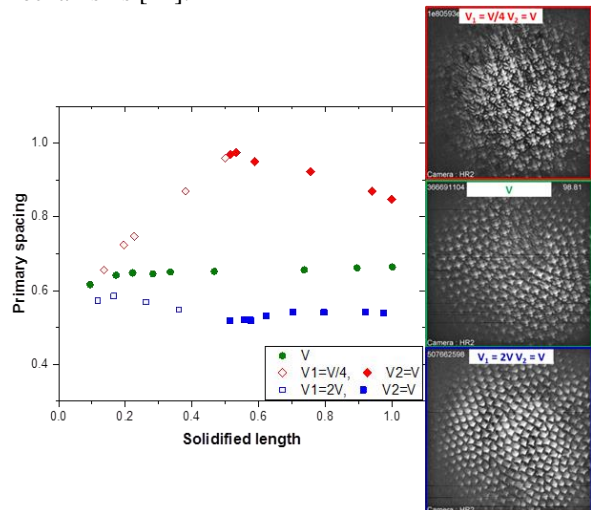


Fig. 7. Primary spacing evolution at V from rest (●), after half-way solidification at V/4 (◆,◇) or 2V (■,□). Axial view snapshots at the end (7.3*7.3mm²). The primary spacing and the solidified length were normalized similarly to fig. 4.

The step-up case (red curve of fig. 7 - $V_{p,1}=V/4$, $V_{p,2}=V$) will be briefly described. Although the primary spacing was not stable at the moment of the pulling rate jump, the interface velocity was precisely the same as the applied pulling velocity (fig. 8). The interface velocity increases rapidly as the applied velocity is changed to V_2 . The interface velocity overshoots significantly, then decreases rapidly, and finally approaches the applied velocity. The change in dendrite tip radius correlates well with the change in interface velocity (inset snapshots in fig. 8): the radius value decreases, exhibiting an overshoot, and finally approaches the steady-state value when the interface velocity coincides with the imposed pulling velocity. No such correlation could be seen between the interface velocity and the primary spacing: it begins to alter only after the interface velocity becomes equal to the applied velocity. Similar results were previously observed in thin samples [19], but in 2D the primary spacing typically decreases because a tertiary arm begins to grow in the direction of the primary dendrite growth. In 3D, very few tertiary branching events (or tip-splitting in the step-down case) were observed and analyses are currently in progress to identify the main sources of spacing adjustment.

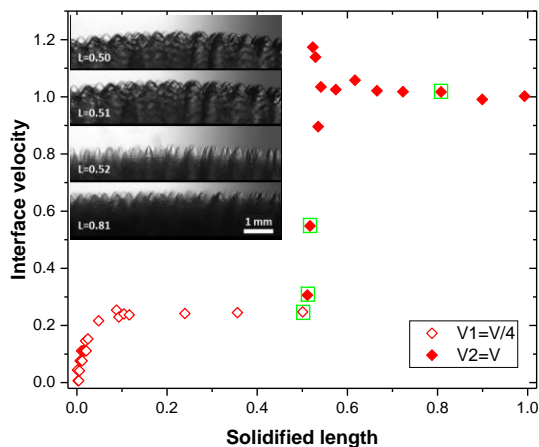


Fig. 8. Interface velocity as function of the solidified length after the pulling rate jump at half-way from $V/4$ to V . Transverse view snapshots corresponding to the green squares. The interface velocity and the solidified length were normalized by the pulling rate V and the crucible length, respectively.

6. Conclusions

This paper reports the preliminary observations and analysis obtained during the second ISS campaign of DECLIC-DSI, dedicated to the *in situ* and real time observation of interfacial microstructure during 3D

directional solidification in diffusive transport conditions using an organic transparent alloy.

The first ISS campaign took place between March 2010 and March 2011 with a SCN-0.24wt% camphor alloy, and it allowed exploration of the full range of microstructures and produced very interesting results. However, most of the analyses were conducted in the cellular or weakly dendritic regimes. The second spatial campaign, DSI-R, realized using a SCN-0.46wt% camphor alloy between October 2017 and November 2018, was focused on investigating the formation of well-developed dendritic patterns which are of direct technological relevance for the solidification and casting industry. The experiments briefly reported in this paper address mainly two questions:

- i) What is the fundamental science of sidebranching formation and what is the critical role of interface anisotropy on cellular and dendritic structures? It includes the measurements of dendrite tip curvature radius as a function of growth parameters, and the study of formation of sidebranches near the dendrite tip.
- ii) What is the fundamental physics that governs the spatio-temporal organization of highly branched dendritic patterns in three-dimensions? It includes for example the topics of dynamics of spacing selection, spatial organization of dendrites, and mechanisms of competition at sub-boundaries (grain structure formation).

The analyses are currently in progress. The results obtained during this ISS flight campaign should be compared to the results obtained during the first ISS campaign to evaluate the effect of nominal solute concentration, to ground-based experiment results to evaluate the effect of convection, to thin sample experiments to evaluate the effect of confinement, and in general to phase-field simulations.

References

- [1] H. Jamgotchian, N. Bergeon, D. Benielli, P. Voge, B. Billia, R. Guerin, Localized microstructures induced by fluid flow in directional solidification, *Phys. Rev. Lett.*, 87 (2001) 6105.
- [2] T. Schenk, H. Nguyen-Thi, J. Gastaldi, G. Reinhart, V. Cristiglio, N. Mangelinck-Noel, H. Klein, J. Hartwig, B. Grushko, B. Billia, J. Baruchel, Application of synchrotron X-ray imaging to the study of directional solidification of aluminium-based alloys, *J. Cryst. Growth*, 275 (2005) 201-208.
- [3] N. Bergeon, F.L. Mota, J. Pereda, D. Tournet, Y. Song, J.M. Debierre, R. Guerin, A. Karma, R. Trivedi, B. Billia, In Situ and Real Time Observation of Microstructure Formation during Directional Solidification of a 3D-alloy: Experiments in the

- DECLIC-DSI, *Int. J. Microgravity Sci. Appl.*, 33 (2016) 6.
- [4] F.L. Mota, Y. Song, J. Pereda, B. Billia, D. Tournet, J.M. Debierre, R. Trivedi, A. Karma, N. Bergeon, Convection effects during bulk transparent alloy solidification in DECLIC-DSI and phase-field simulations in diffusive conditions, *JOM*, 69 (2017) 1280-1288.
- [5] F.L. Mota, N. Bergeon, D. Tournet, A. Karma, R. Trivedi, B. Billia, Initial transient behavior in directional solidification of a bulk transparent model alloy in a cylinder, *Acta Mater.*, 85 (2015) 362-377.
- [6] Y. Song, D. Tournet, F.L. Mota, J. Pereda, B. Billia, N. Bergeon, R. Trivedi, A. Karma, Thermal-field effects on interface dynamics and microstructure selection during alloy directional solidification, *Acta Mater*, 150 (2018) 139-152.
- [7] N. Bergeon, D. Tournet, L. Chen, J.M. Debierre, R. Guerin, A. Ramirez, B. Billia, A. Karma, R. Trivedi, Spatiotemporal Dynamics of Oscillatory Cellular Patterns in Three-Dimensional Directional Solidification, *Phys. Rev. Lett.*, 110 (2013) 6102.
- [8] J. Pereda, F.L. Mota, L. Chen, B. Billia, D. Tournet, Y. Song, J.M. Debierre, R. Guérin, A. Karma, R. Trivedi, N. Bergeon, Experimental observation of oscillatory cellular patterns in three-dimensional directional solidification, *Phys. Rev. E*, 95 (2017) 2803.
- [9] D. Tournet, J.-M. Debierre, Y. Song, F.L. Mota, N. Bergeon, R. Guérin, R. Trivedi, B. Billia, A. Karma, Oscillatory cellular patterns in three-dimensional directional solidification, *Phys. Rev. E*, 92 (2015) 2401.
- [10] R. Trivedi, W. Kurz, Dendritic growth, *Int. Mater. Rev.*, 39 (1994) 49-74.
- [11] A. Karma, W.J. Rappel, Quantitative phase-field modeling of dendritic growth in two and three dimensions, *Phys. Rev. E*, 57 (1998) 4323-4349.
- [12] R. Marcout, G. Raymond, B. Martin, G. Cambon, B. Zappoli, F. Duclos, S. Barde, D. Beysens, Y. Garrabos, C. Lecoutre, B. Billia, N. Bergeon, N. Mangelinck, DECLIC: a facility to investigate fluids and transparent materials in microgravity conditions in ISS, in: 57th International Astronautical Congress, Valencia, Spain, 2006.
- [13] G. Pont, S. Barde, B. Zappoli, F. Duclos, Y. Garrabos, C. Lecoutre, D. Beysens, B. Billia, N. Bergeon, N. Mangelinck, R. Marcout, D. Blonde, DECLIC: a facility to study crystallization and critical fluids, in: 60th International Astronautical Congress, Daejeon, Republic of Korea, 2009.
- [14] N. Bergeon, C. Weiss, N. Mangelinck-Noel, B. Billia, Interferometric method for the analysis of dendrite growth and shape in 3D extended patterns in transparent alloys, *Trans. Ind. Inst. Met.*, 62 (2009) 455-460.
- [15] H. Jamgotchian, N. Bergeon, D. Benielli, P. Voge, B. Billia, In situ observation and interferometric characterization of solid-liquid interface morphology in directionally growing transparent model systems, *J. Microsc.*, 203 (2001) 119-127.
- [16] J. Pereda, F.L. Mota, B. Billia, Y. Song, J.M. Debierre, A. Karma, R. Trivedi, N. Bergeon, Evolution of primary spacing during directional solidification of transparent bulk samples conducted on DECLIC-DSI, in: 5th Decennial International Conference on Solidification Processing, Old Windsor, 2017.
- [17] S.H. Han, R. Trivedi, Primary Spacing Selection in Directionally Solidified Alloys, *Acta Metall. Mater.*, 42 (1994) 25-41.
- [18] V. Seetharaman, M.A. Eshelman, R. Trivedi, Cellular spacings—II. Dynamical studies, *Acta Metall.*, 36 (1988) 1175-1185.
- [19] K. Somboonsuk, R. Trivedi, Dynamical Studies of Dendritic Growth, *Acta Metall.*, 33 (1985) 1051-1060.
- [20] W. Losert, B.Q. Shi, H.Z. Cummins, J.A. Warren, Spatial period-doubling instability of dendritic arrays in directional solidification, *Phys. Rev. Lett.*, 77 (1996) 889-891.
- [21] Y. Song, S. Akamatsu, S. Bottin-Rousseau, A. Karma, Propagative selection of tilted array patterns in directional solidification, *Phys Rev Mater*, 2 (2018).